Electronic Supplementary Information

Room-temperature rapid synthesis of hierarchically porous ZIF-93 for effective adsorption of volatile organic compounds

Haiqi Zhang[a], Kaikai Zhao[a], Weibiao Guo[a], Kuan Liang[a], Jingjing Li[a], Xu Li[d], Qianjun Deng[a], Xuejun Xu[a], Huixia Chao[c], Hongxia Xi[b,*], Chongxiong Duan[a,*]

[a] School of Materials Science and Hydrogen Engineering, Foshan University, Foshan, 528231, China.

[b] School of Chemistry and Chemical Engineering, South China University of Technology, Guangzhou, 510640, China.

[c] Guangxi Key Laboratory of Green Chemical Materials and Safety Technology, College of Petroleum and Chemical Engineering, Beibu Gulf University, Qinzhou 535011, China.

[d] Key Laboratory of Nuclear Solid-State Physics Hubei Province, School of Physics and Technology, Wuhan University, Wuhan 430072, China.

Calculation

Space-Time Yields (STYs)

The space-time yields (STYs, in units of $kg \cdot m^{-3} \cdot d^{-1}$) data were obtained to predict the value of hierarchical porous ZIF-93 for practical applications. The STY was calculated using the following equation:

$$STY = \left(\frac{m_1}{V_{solution} \tau} \right) \times 1.44 \times 10^6$$

Where m_1 is representative of the dried mass (g) for the as-synthesized hierarchically porous ZIF-93 powder obtained from rapid synthesis at RT, $V_{solution}$ is the total volume (cm^3) for the total solution, and τ is the stirring time (min).

Table S1. Elemental content of C, O, N, and Zn of hierarchical porous ZIF-93_A*t* (*t*=1, 10, 60).

Samples	C (wt. %)	O (wt. %)	N (wt. %)	Zn (wt. %)
ZIF-93_A1	39.48	23.48	22.18	14.86
ZIF-93_A10	35.80	19.48	28.76	15.96
ZIF-93_A60	36.99	16.51	28.44	18.06

Table S2. Porosity properties of the as-synthesized ZIF-93 samples.

Samples	S_{BET} [$m^2\ g^{-1}$]	S_{micro} [$m^2\ g^{-1}$]	S_{ext} [$m^2\ g^{-1}$]	V_t [$cm^3\ g^{-1}$]	V_{micro} [$cm^3\ g^{-1}$]	V_{meso} [$cm^3\ g^{-1}$]	Pore size [nm]	STYs [$kg\ m^{-3}\ d^{-1}$]
ZIF-93_Activated	1071	954	117	0.51	0.36	0.15	6.7	3570
ZIF-93_$ZnNO_3$	519	429	90	0.38	0.16	0.22	8.7	4468
ZIF-93_$ZnSO_4$	684	601	83	0.36	0.23	0.13	8.4	4883
ZIF-93_KOH	849	740	109	0.45	0.28	0.17	6.9	4143
ZIF-93_$NH_3 \cdot H_2O$	794	720	74	0.44	0.27	0.17	13.4	2874
Zn^{2+}/almeIm=1/0.5	66	16	50	0.42	0.007	0.413	26.5	3000
Zn^{2+}/almeIm=1/4	1049	958	91	0.50	0.37	0.13	4.7	5586
Zn^{2+}/H_2O=1/5560	1224	1192	32	0.54	0.46	0.08	5.7	1244
Zn^{2+}/H_2O=1/1390	946	919	27	0.43	0.35	0.08	5.8	9670
pH=6	1006	889	117	0.51	0.33	0.18	8.0	-

pH=7	978	874	104	0.43	0.33	0.10	4.4	-
pH=8	771	693	78	0.39	0.26	0.13	7.9	-
pH=9	453	324	129	0.58	0.12	0.46	13.7	-
pH=10	651	499	152	0.72	0.19	0.53	13.7	-

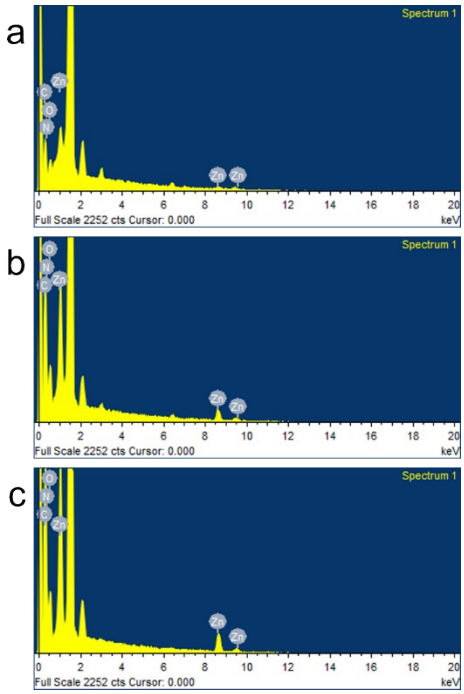

Fig. S1 The mass ratio and molar ratio of C/O/N/Zn in the (a) ZIF-93_A1, (b) ZIF-93_A10, and (c) ZIF-93_A60.

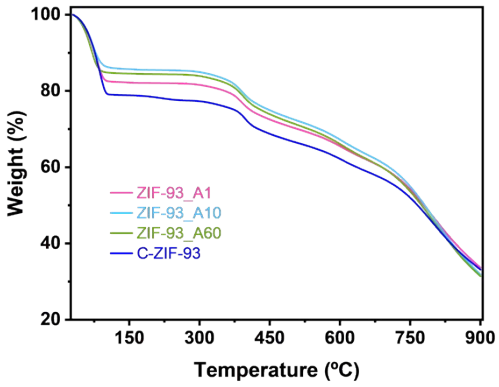

Fig. S2 TGA curves of ZIF-93_At and C-ZIF-93 samples.

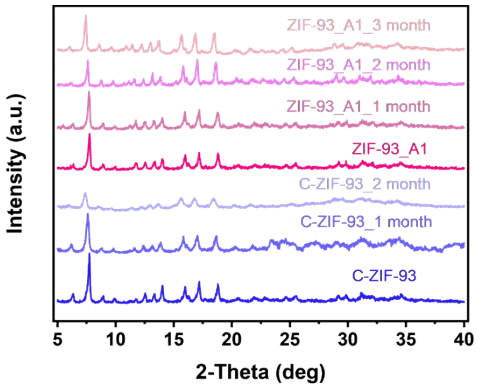

Fig. S3 XRD patterns of the as-synthesized ZIF-93 after soaking in water at different times.

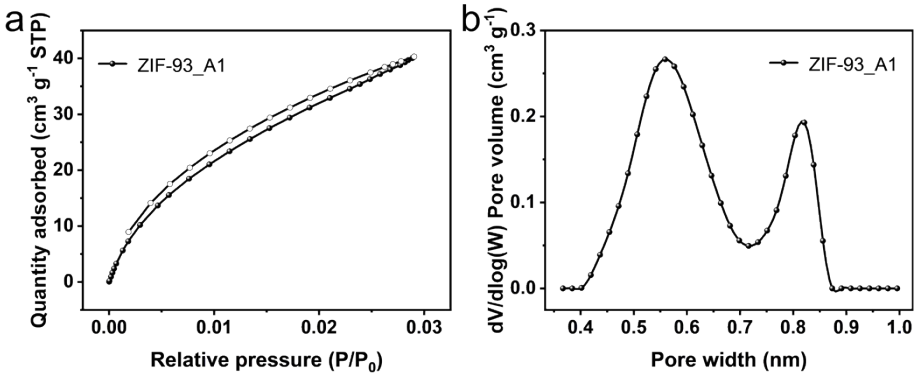

Fig. S4 (a) CO_2 adsorption-desorption isotherms and (b) PSDs of ZIF-93_A1 samples.

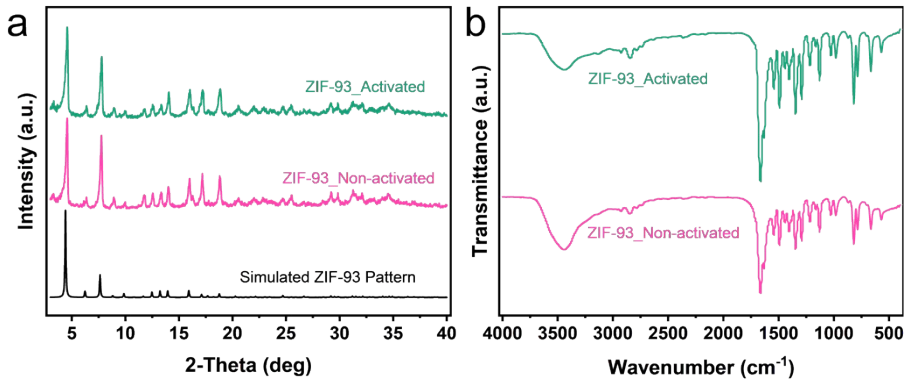

Fig. S5 (a) Powder XRD patterns of ZIF-93_Activated and ZIF-93_Non-activated samples, and simulated XRD pattern of ZIF-93. (b) FT-IR spectra of the as-synthesized ZIF-93_Activated and ZIF-93_Non-activated samples.

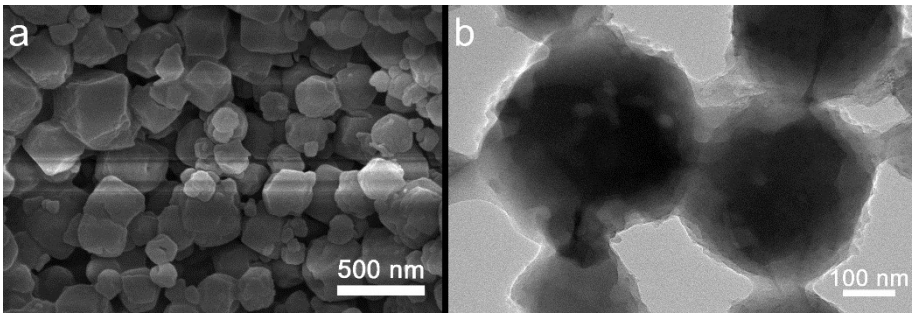

Fig. S6 SEM and TEM images of ZIF-93_Activated samples.

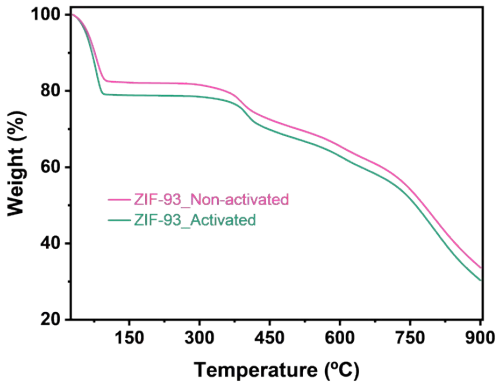

Fig. S7 TGA curves of ZIF-93_Activated and ZIF-93_Non-activated samples.

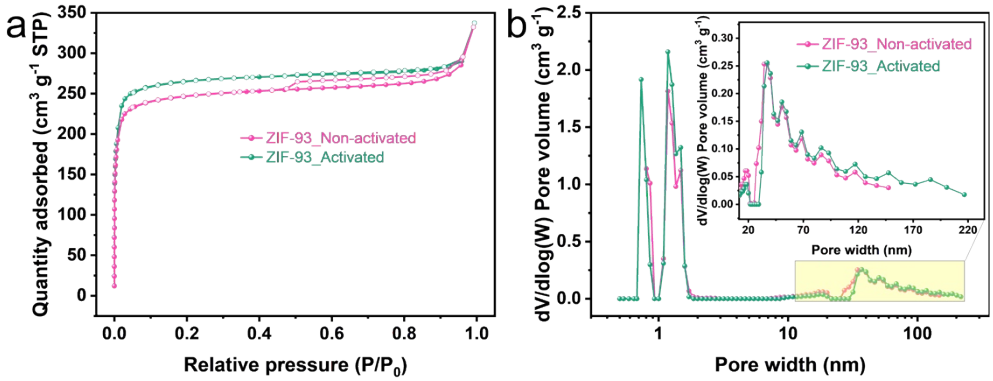

Fig. S8 (a) N_2 adsorption-desorption isotherms and (b) PSDs of ZIF-93_Activated and ZIF-93_Non-activated samples.

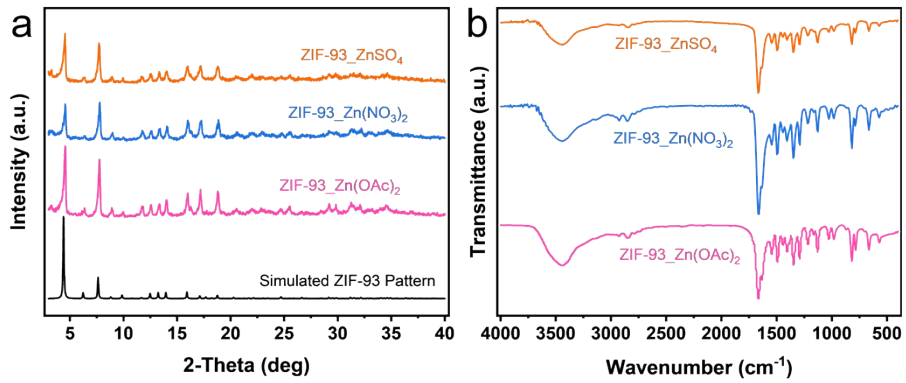

Fig. S9 (a) Powder XRD patterns of ZIF-93_$Zn(OAc)_2$, ZIF-93_$Zn(NO_3)_2$, ZIF-93_$ZnSO_4$ samples, and simulated XRD pattern of ZIF-93. (b) FT-IR spectra of the as-synthesized ZIF-93_$Zn(OAc)_2$, ZIF-93_$Zn(NO_3)_2$, and ZIF-93_$ZnSO_4$ samples.

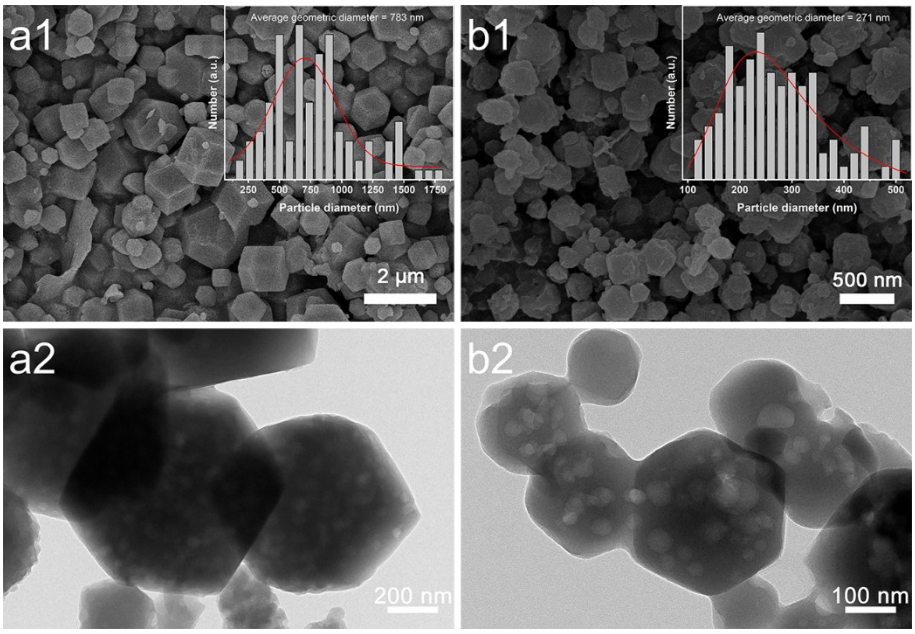

Fig. S10 SEM and TEM images of ZIF-93 samples: (a) ZIF-93_$ZnSO_4$, (b) ZIF-93_$Zn(NO_3)_2$.

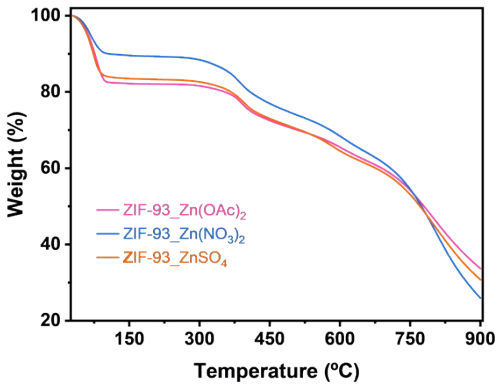

Fig. S11 TGA curves of ZIF-93_$Zn(OAc)_2$, ZIF-93_$Zn(NO_3)_2$, and ZIF-93_$ZnSO_4$ samples.

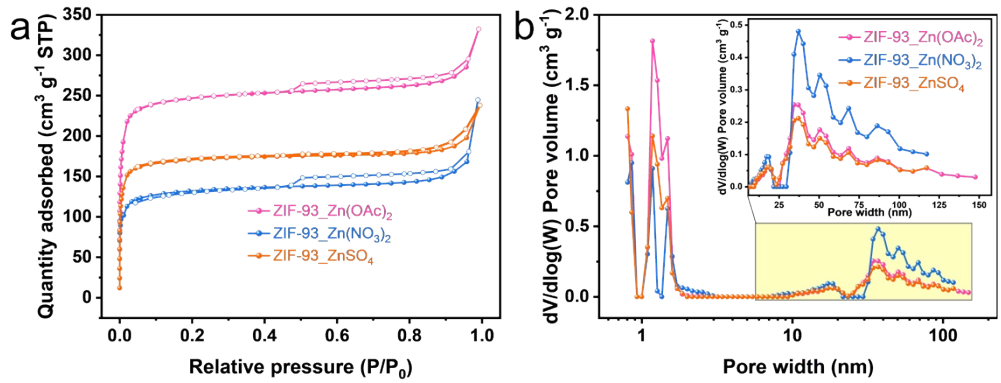

Fig. S12 (a) N_2 adsorption-desorption isotherms and (b) PSDs of ZIF-93_Zn(OAc)$_2$, ZIF-93_Zn(NO$_3$)$_2$, and ZIF-93_ZnSO$_4$ samples.

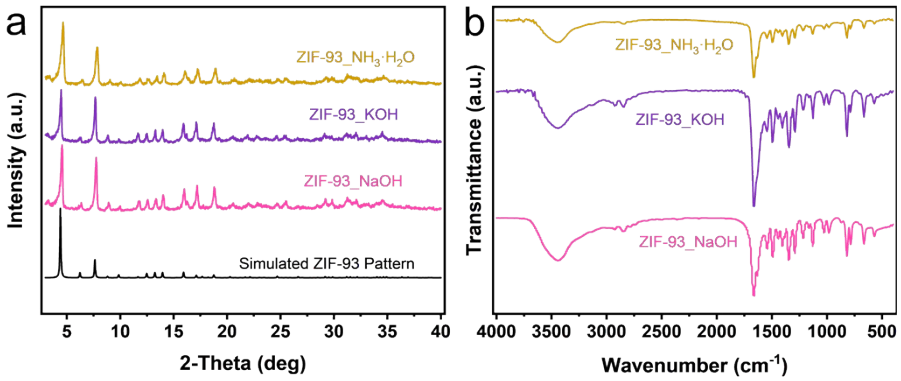

Fig. S13 (a) Powder XRD patterns of ZIF-93_NaOH, ZIF-93_KOH, ZIF-93_NH$_3$·H$_2$O samples and simulated XRD pattern of ZIF-93. (b) FT-IR spectra of the as-synthesized ZIF-93_NaOH, ZIF-93_KOH, and ZIF-93_NH$_3$·H$_2$O samples.

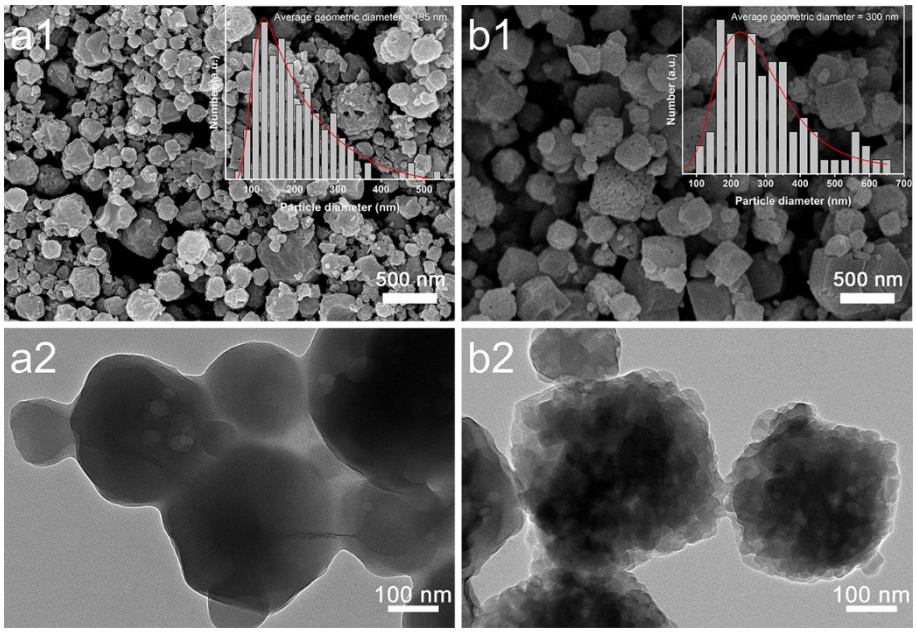

Fig. S14 SEM and TEM images of ZIF-93 samples: (a) ZIF-93_NH$_3$·H$_2$O, (b) ZIF-93_KOH.

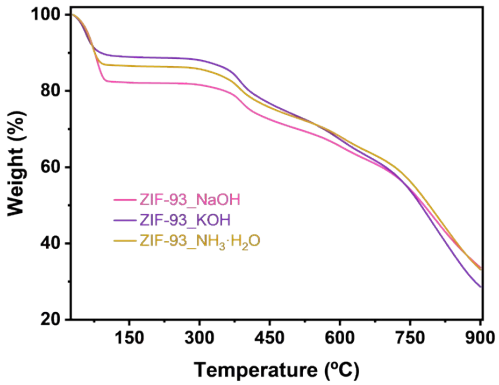

Fig. S15 TGA curves of ZIF-93_NaOH, ZIF-93_KOH, and ZIF-93_NH_3·H_2O samples.

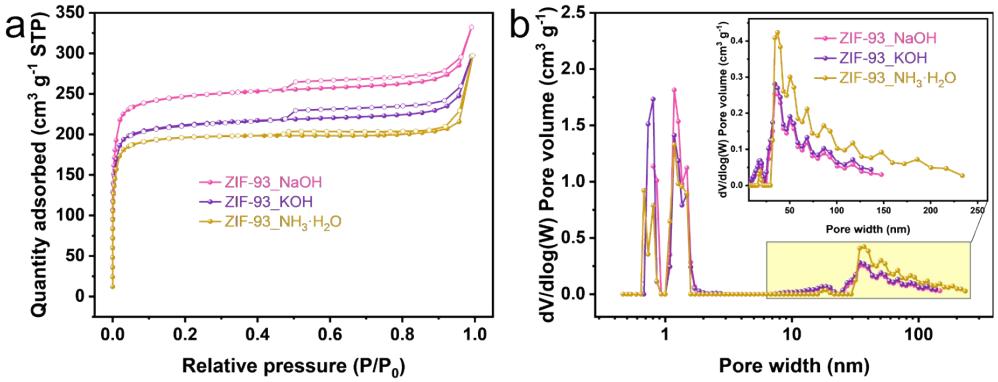

Fig. S16 (a) N_2 adsorption-desorption isotherms and (b) PSDs of ZIF-93_NaOH, ZIF-93_KOH, and ZIF-93_NH_3·H_2O samples.

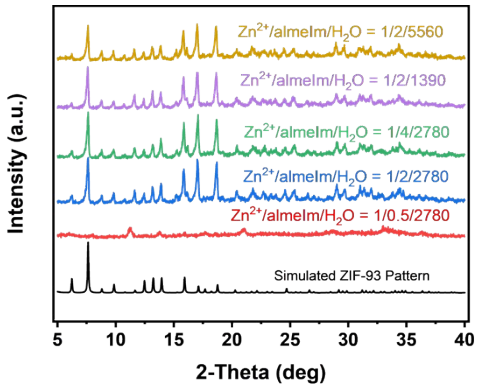

Fig. S17 Powder XRD patterns of ZIF-93 samples with different molar ratios and simulated XRD pattern of ZIF-93.

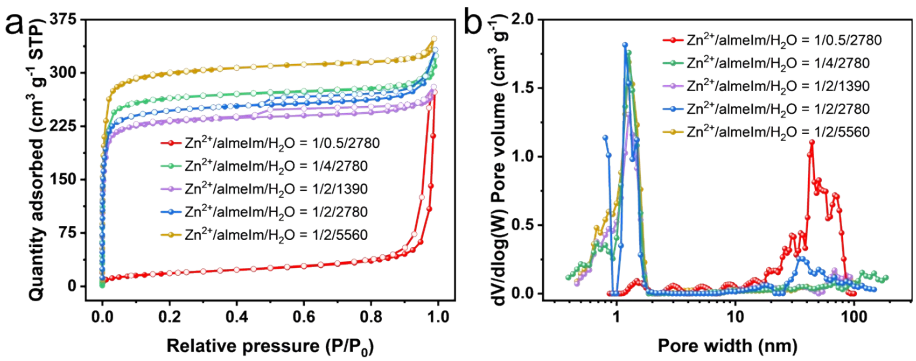

Fig. S18 (a) N_2 adsorption-desorption isotherms and (b) PSDs of ZIF-93 samples with different molar ratios.

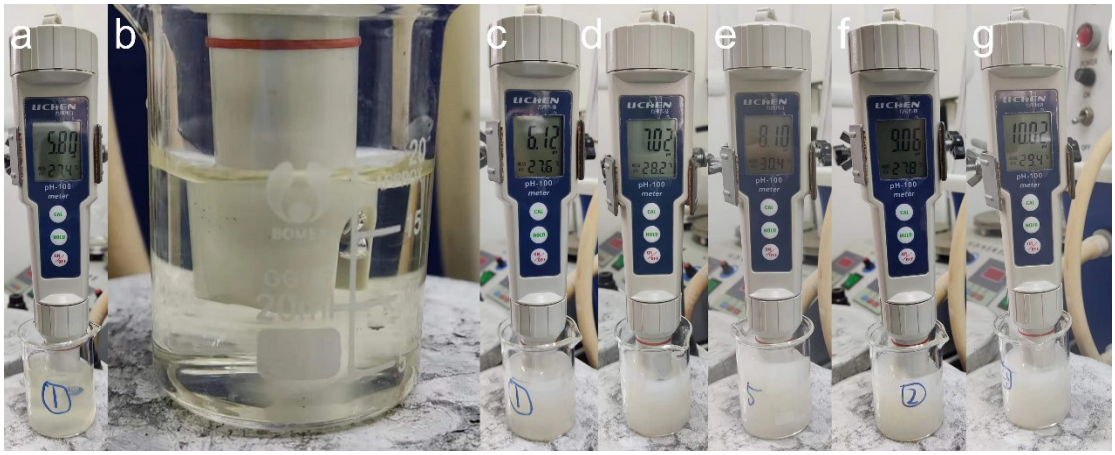

Fig. S19 Pictures of different pH in the synthesis of ZIF-93: (a) Initial pH, (b) pH=5, (c) pH=6, (d) pH=7, (e) pH=8, (f) pH=9, and (g) pH=10.

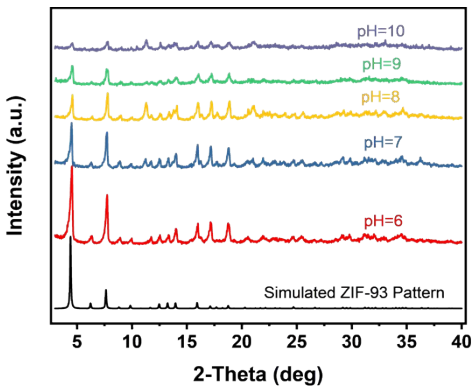

Fig. S20 Powder XRD patterns of ZIF-93 samples with different pH and simulated XRD pattern of ZIF-93.

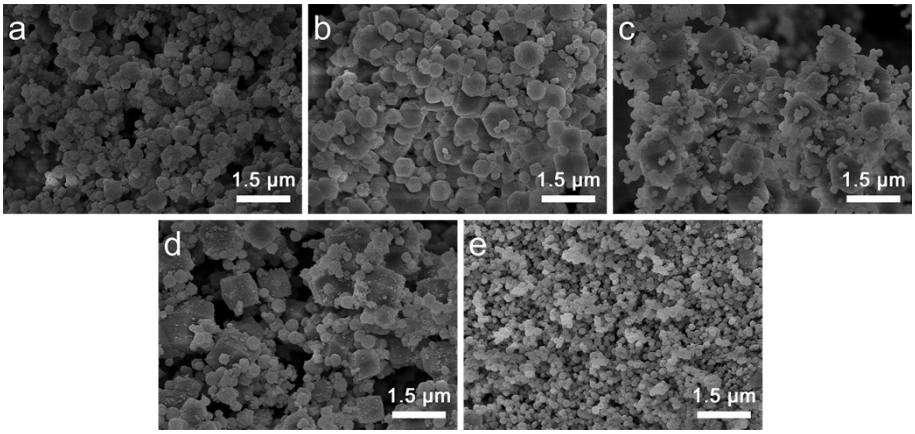

Fig. S21 SEM images of ZIF-93 samples with different pH: (a) pH=6, (b) pH=7, (c) pH=8, (d) pH=9, and (e) pH=10.

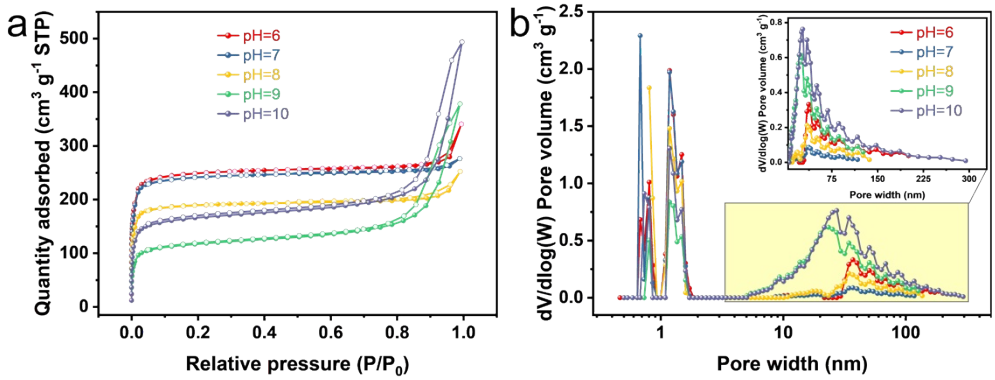

Fig. S22 (a) N_2 adsorption-desorption isotherms and (b) PSDs of ZIF-93 samples with different pH.

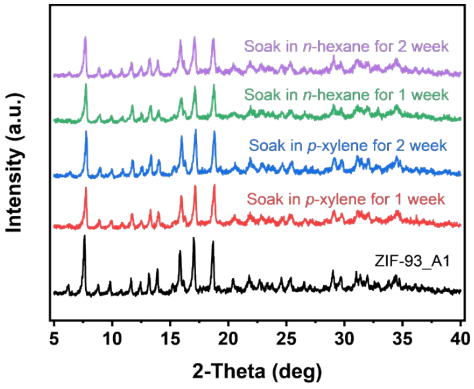

Fig. S23 XRD patterns of the as-synthesized ZIF-93 after soaking in VOCs at different times.

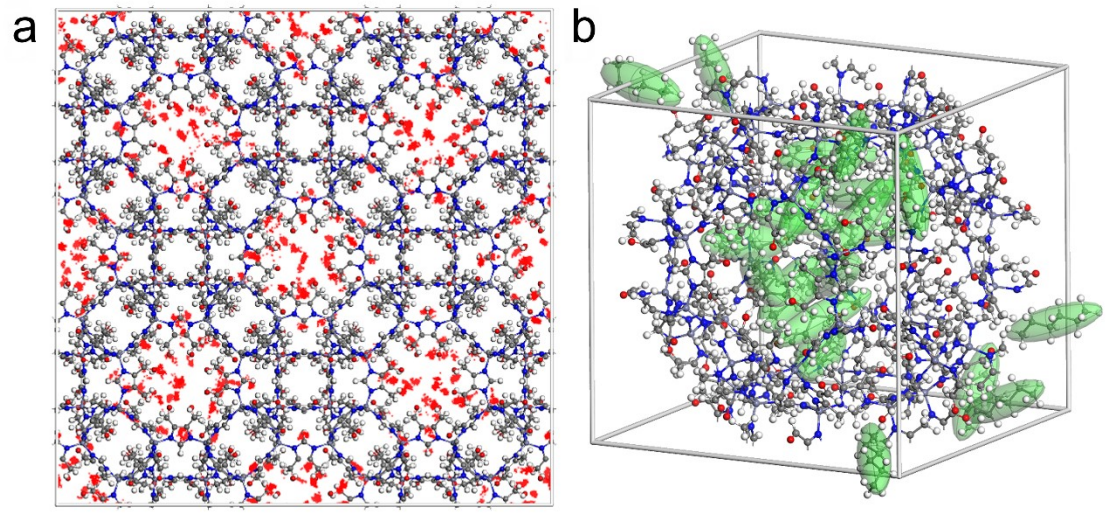

Fig. S24 (a) Adsorption density distribution and (b) adsorption distribution of *n*-hexane on ZIF-93 at a relative pressure of 0.3 (P/P_0).

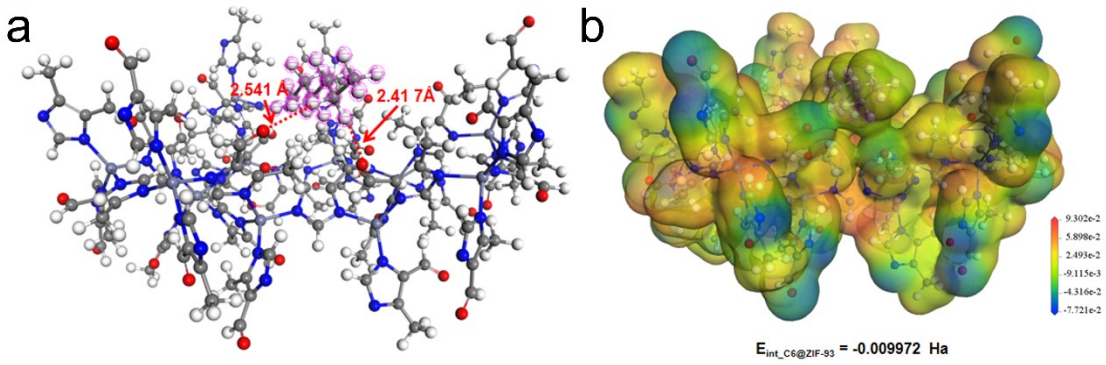

Fig. S25 (a) Adsorption sites and (b) electrostatic potential of *n*-hexane on ZIF-93.